Entanglement generation and degradation by passive optical devices

S. Scheel and D.-G. Welsch
Theoretisch-Physikalisches Institut, Friedrich-Schiller-Universität Jena, Max-Wien-Platz 1, D-07743 Jena, Germany
(Received 30 March 2001; published 16 November 2001)

The influence of losses in the interferometric generation and the transmission of continuous-variable entangled light is studied, with special emphasis on Gaussian states. Based on the theory of quantum-state transformation at absorbing dielectric devices, the amount of entanglement is quantified by means of the relative-entropy measure. Upper bounds of entanglement and the distance to the set of separable Gaussian states are calculated. Compared with the distance measure, the bounds can substantially overestimate the entanglement. In particular, they do not show the drastic decrease of entanglement with increasing mean photon number, as does the distance measure.

DOI: 10.1103/PhysRevA.64.063811 PACS number(s): 42.50.Lc, 03.67.−a, 42.25.Bs, 42.79.−e

I. INTRODUCTION

Entangled quantum states that exist generically in infinite-dimensional Hilbert spaces have been of increasing interest (see, for example, [1]). Typical examples are Gaussian states such as two-mode squeezed vacuum states, which are the states commonly used in quantum communication of continuous-variable systems, e.g., quantum teleportation [2–4] and quantum dense coding [5–7]. In practice, necessarily existing dissipative environments spoil the quantum-state purity and coherence, and the question arises as to the amount of entanglement that is really available.

Unfortunately, computation of the amount of entanglement of mixed states in infinite-dimensional Hilbert spaces is as yet impossible in practice. It typically involves minimizations over a very large ($\to\infty$) number of parameters, as is the case for the entropy of formation as well as for the distance to the set of all separable quantum states measured by either the relative entropy or Bures' metric [8]. It is, however, possible to derive upper bounds on the entanglement content [9] by using the convexity property of the relative entropy. For Gaussian states, however, it is possible to derive an upper bound based on the distance to the set of separable Gaussian states that is far better than the convexity bound and may be very useful for estimation of the entanglement degradation in continuous-variable quantum communication. In particular, it reveals the ultimate limits for quantum-mechanical transmission of information through noisy channels.

The aim of the present article is to study the generation and processing of entangled Gaussian states of light by absorbing devices. In Sec. II the influence of losses in the interferometric entanglement generation at a beam splitter is studied. A typical situation in quantum communication is considered in Sec. III, in which the entanglement degradation of a two-mode squeezed vacuum (TMSV) state transmitted through a noisy communication channel, say, two lossy optical fibers, is examined. Some concluding remarks are given in Sec. IV.

II. ENTANGLEMENT GENERATION BY MIXING SQUEEZED VACUA AT A BEAM SPLITTER

A. Lossless beam splitters

Let us first consider the case of a lossless beam splitter and (quasi)monochromatic light of (mid-)frequency ω (Fig. 1). It is well known [10–15] that a lossless beam splitter transforms the operators of the incoming modes $\hat{a}_1(\omega)$ and $\hat{a}_2(\omega)$ to the operators of the outgoing modes $\hat{b}_1(\omega)$ and $\hat{b}_2(\omega)$ according to

$$\begin{pmatrix} \hat{b}_1(\omega) \\ \hat{b}_2(\omega) \end{pmatrix} = \mathbf{T}(\omega) \begin{pmatrix} \hat{a}_1(\omega) \\ \hat{a}_2(\omega) \end{pmatrix}, \tag{1}$$

where $\mathbf{T}(\omega)$ is the unitary characteristic transformation matrix of the beam splitter. Equivalently, the operators can be left unchanged and instead the density operator is transformed with the inverse matrix $\mathbf{T}^{-1}(\omega)=\mathbf{T}^{+}(\omega)$ according to

$$\hat{\varrho}_{\rm out} = \hat{\varrho}_{\rm in}\left[\mathbf{T}^{+}(\omega) \begin{pmatrix} \hat{a}_1(\omega) \\ \hat{a}_2(\omega) \end{pmatrix}, \mathbf{T}^{\rm T}(\omega) \begin{pmatrix} \hat{a}_1^{\dagger}(\omega) \\ \hat{a}_2^{\dagger}(\omega) \end{pmatrix} \right]. \tag{2}$$

Let each of the two incoming modes be prepared in a squeezed vacuum state, i.e.,

$$\hat{\varrho}_{\rm in} = |\Psi_{\rm in}\rangle\langle\Psi_{\rm in}| \tag{3}$$

where

$$|\Psi_{\rm in}\rangle = \hat{S}_1\hat{S}_2|0,0\rangle, \tag{4}$$

with $\hat{S}_i (i=1,2)$ being the (single-mode) squeeze operator

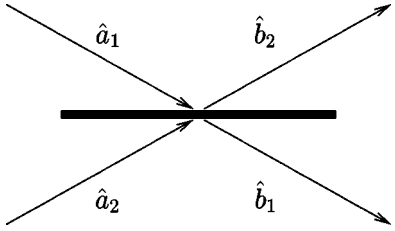

FIG. 1. Squeezed states $|\psi_1\rangle$ and $|\psi_2\rangle$ impinging on a beam splitter producing entangled light beams.

$$\hat{S}_i=\exp\left[-\frac{1}{2}(\xi_i\hat{a}_i^{\dagger 2}-\xi_i^*\hat{a}_i^2)\right]=\exp\left(-\frac{1}{2}q_i\hat{a}_i^{\dagger 2}\right)$$
$$\times(1-|q_i|^2)^{(2\hat{n}_i+1)/4}\exp\left(\frac{1}{2}q_i^*\hat{a}_i^2\right) \tag{5}$$

($q_i=\tanh|\xi_i|e^{i\phi_i}$, $\phi_i=\arg\xi_i$). Here, the second equality follows from general disentangling theorems [16,17]. By Eq. (2), the output quantum state is

$$\hat{\varrho}_{\rm out}=|\Psi_{\rm out}\rangle\langle\Psi_{\rm out}|, \tag{6}$$

where

$$|\Psi_{\rm out}\rangle=[(1-|q_1|^2)(1-|q_2|^2)]^{1/4}\exp\left[-\frac{1}{2}q_1(T_{11}\hat{a}_1^\dagger+T_{21}\hat{a}_2^\dagger)^2-\frac{1}{2}q_2(T_{12}\hat{a}_1^\dagger+T_{22}\hat{a}_2^\dagger)^2\right]|0,0\rangle. \tag{7}$$

The T_{ij} are the elements of the characteristic transformation matrix $\mathbf{T}$ (at the chosen mid-frequency), which can be given, without loss of generality, in the form

$$\mathbf{T}=\begin{pmatrix} T & R \\ -R^* & T^* \end{pmatrix}, \tag{8}$$

with $T=|T|e^{i\phi_T}$ and $R=|R|e^{i\phi_R}$ being the (complex) transmission and reflection coefficients of the beam splitter.

From inspection of Eq. (6) it is seen that the preparation of an entangled state is controlled by the parameter

$$\xi_{12}=q_1T_{11}T_{21}+q_2T_{12}T_{22}=-q_1TR^*+q_2RT^*. \tag{9}$$

When $\xi_{12}=0$ is valid, then the output state is separable. This is the case for $\phi_1-\phi_2+2(\phi_T-\phi_R)=0$ and $|q_1|=|q_2|$. On the other hand, if again $|q_1|=|q_2|=|q|$ but $\phi_1-\phi_2+2(\phi_T-\phi_R)=\pm\pi$, then for $|TR|=1/2$ the output quantum state is just a TMSV state,

$$|\Psi_{\rm out}\rangle=|{\rm TMSV}\rangle=\sqrt{1-|q|^2}\exp[-q\hat{a}_1^\dagger\hat{a}_2^\dagger]|0,0\rangle, \tag{10}$$

where

$$q=|q|^{i(\phi_2+\phi_R-\phi_T)}=-|q|e^{i(\phi_1+\phi_T-\phi_R)}. \tag{11}$$

Since, according to Eq. (6), the output quantum state is a pure state, entanglement is uniquely measured by the von Neumann entropy of the (reduced) quantum state of either of the output modes,

$$E(\hat{\varrho}_{\rm out})=S_{1(2)}=-{\rm Tr}[\hat{\varrho}_{1(2)}\ln\hat{\varrho}_{1(2)}], \tag{12}$$

where $\hat{\varrho}_{1(2)}$ denotes the (reduced) output density operator of mode 1 (2), which is obtained by tracing $\hat{\varrho}_{\rm out}$ with respect to mode 2 (1). Note that using squeezed coherent states instead of squeezed vacuum states does not change the entanglement. This is due to the fact that coherent shifts are unitary operations on subsystems which leave any entanglement measure invariant.

B. Lossy beam splitters

In practice there are always some losses and things get slightly more complicated. The SU(2) group transformation in Eq. (1) has to be replaced by an SU(4) group transformation, where the unitary transformation acts in the product Hilbert space of the field modes and the device modes [18–20]. As a result, Eqs. (1) and (2), respectively, have to be replaced by

$$\hat{\boldsymbol{\beta}}(\omega)=\boldsymbol{\Lambda}(\omega)\hat{\boldsymbol{\alpha}}(\omega) \tag{13}$$

and

$$\hat{\varrho}_{\rm out}^{\rm (F)}={\rm Tr}^{\rm (D)}\hat{\varrho}_{\rm in}[\boldsymbol{\Lambda}^+(\omega)\hat{\boldsymbol{\alpha}}(\omega),\boldsymbol{\Lambda}^{\rm T}(\omega)\hat{\boldsymbol{\alpha}}^\dagger(\omega)], \tag{14}$$

where the "four-vector" notation $\hat{\boldsymbol{\alpha}}(\omega)$ for abbreviating the list of operators $\hat{a}_1(\omega)$, $\hat{a}_2(\omega)$, $\hat{g}_1(\omega)$, and $\hat{g}_2(\omega)$ [and $\hat{\boldsymbol{\beta}}(\omega)$ accordingly] has been used. The SU(4) group element $\boldsymbol{\Lambda}(\omega)$ is expressed in terms of the characteristic transformation and absorption matrices $\mathbf{T}(\omega)$ and $\mathbf{A}(\omega)$ of the beam splitter as

$$\boldsymbol{\Lambda}(\omega)=\begin{pmatrix} \mathbf{T}(\omega) & \mathbf{A}(\omega) \\ -\mathbf{S}(\omega)\mathbf{C}^{-1}(\omega)\mathbf{T}(\omega) & \mathbf{C}(\omega)\mathbf{S}^{-1}(\omega)\mathbf{A}(\omega) \end{pmatrix} \tag{15}$$

with the commuting positive Hermitian matrices

$$\mathbf{C}(\omega)=\sqrt{\mathbf{T}(\omega)\mathbf{T}^+(\omega)},\quad \mathbf{S}(\omega)=\sqrt{\mathbf{A}(\omega)\mathbf{A}^+(\omega)}. \tag{16}$$

From the above, the output density matrix in the Fock basis can be given in the form of (Appendix A)

$$\langle m_1,m_2|\hat{\varrho}_{\rm out}^{\rm (F)}|n_1,n_2\rangle = \sqrt{\frac{(1-|q_1|^2)(1-|q_2|^2)}{m_1!m_2!n_1!n_2!}}(-1)^{m_1+m_2+n_1+n_2} \times\sum_{g_1,g_2=0}^{\infty}\frac{1}{g_1!g_2!}H^{\mathbf{M}}_{m_1,m_2,g_1,g_2}(\mathbf{0})H^{*\mathbf{M}}_{n_1,n_2,g_1,g_2}(\mathbf{0}), \tag{17}$$

where $H_n^{\mathbf{M}}(\mathbf{0})$ denotes the Hermite polynomial of four variables with zero argument, generated by the symmetric matrix $\mathbf{M}$ with elements

$$M_{ij}=q_1\Lambda_{i1}\Lambda_{j1}+q_2\Lambda_{i2}\Lambda_{j2}. \tag{18}$$

Note that in Eq. (17) it is assumed that the device is prepared in the ground state.

In order to quantify the entanglement content of a mixed state $\hat{\varrho}$, such as $\hat{\varrho}_{\rm out}^{\rm (F)}$ in Eq. (17), we make use of the relative entropy measuring the distance of the state to the set $\mathcal{S}$ of all separable states $\hat{\sigma}$ [8],

$$E(\hat{\varrho})=\min_{\hat{\sigma}\in\mathcal{S}}{\rm Tr}[\hat{\varrho}(\ln\hat{\varrho}-\ln\hat{\sigma})]. \tag{19}$$

For pure states this measure reduces to the von Neumann entropy (12) of either of the subsystems, which can be computed by means of Schmidt decomposition of the continuous-variable state [21]. It is also known that when the quantum state has the Schmidt form

$$\hat{\varrho}=\sum_{n,m} C_{n,m}|\phi_n,\psi_n\rangle\langle\phi_m,\psi_m|, \tag{20}$$

then the amount of entanglement measured by the relative entropy is given by [22,23]

$$E(\hat{\varrho})=-\sum_{n} C_{n,n}\ln C_{n,n}-S(\hat{\varrho}). \tag{21}$$

Unfortunately, there is no closed solution of Eq. (19) for arbitrary mixed states. Nevertheless, upper bounds on the entanglement can be calculated [9], representing the quantum state under study in terms of states in Schmidt decomposition and using the convexity of the relative entropy,

$$E\left(\sum_{n} p_n\hat{\varrho}_n\right)\leqslant\sum_{n} p_nE(\hat{\varrho}_n),\quad \sum_{n} p_n=1. \tag{22}$$

Applying the method to the output quantum state in Eq. (17), i.e., rewriting it in the form of

$$\begin{aligned}\hat{\varrho}_{\rm out}^{(\rm F)}&=\sum_{k,l=0}^{\infty} C_{k,l,0}|k,k\rangle\langle l,l|+\sum_{m=1}^{\infty}\sum_{k,l=0}^{\infty} C_{k,l,m}|k+m,k\rangle\\&\otimes\langle l+m,l|+\sum_{m=1}^{\infty}\sum_{k,l=0}^{\infty} C_{k,l,m}|k,k+m\rangle\langle l,l+m|\\&=p_0\hat{\varrho}_0+\sum_{m=1}^{\infty} p_m\hat{\varrho}_{m,1}+\sum_{m=1}^{\infty} p_m\hat{\varrho}_{m,2},\end{aligned} \tag{23}$$

the inequality (22) leads to

$$E(\hat{\varrho}_{\rm out}^{(\rm F)})\leqslant p_0E(\hat{\varrho}_0)+\sum_{m=1}^{\infty} p_m[E(\hat{\varrho}_{m,1})+E(\hat{\varrho}_{m,2})], \tag{24}$$

where $E(\hat{\varrho}_0)$, $E(\hat{\varrho}_{m,1})$, and $E(\hat{\varrho}_{m,2})$ can be determined according to Eq. (21). In the numerical calculation we have used the dielectric-plate model of a beam splitter, taking the **T** and **A** matrices from [20,24]. The result is illustrated in Fig. 2, which shows the dependence on the plate thickness of the upper bound of the attainable entanglement. The oscillations are due to phase matching and phase mismatch at certain beam splitter thicknesses [cf. Eq. (9)]. Note that the local minima of the curve for the lossy beam splitter never go down to zero as do the corresponding minima of the curve for the lossless beam splitter. This obviously reflects the fact that the result for the lossless beam splitter is exact, whereas that for the lossy beam splitter is only an upper bound.

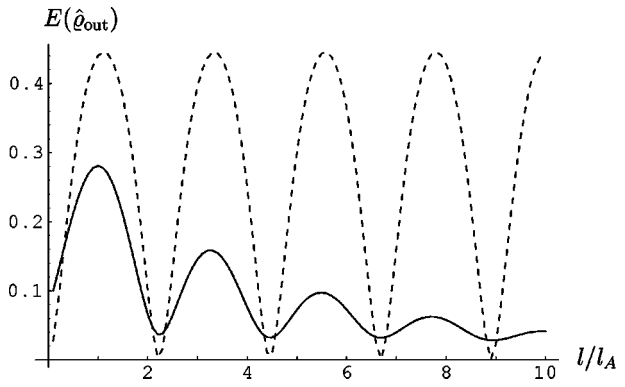

FIG. 2. Entanglement produced at a lossless beam splitter with refractive index $n=1.41$ (dashed curve) as a function of the beam splitter thickness l. The full curve shows the upper bound of the entanglement produced at a lossy beam splitter with $n=1.41+0.1i$. The squeezing parameters chosen are $q_1=q_2=0.5$.

III. ENTANGLEMENT DEGRADATION IN TMSV TRANSMISSION THROUGH LOSSY OPTICAL FIBERS

Let us now turn to the problem of entanglement degradation in transmission of light prepared in a TMSV state through absorbing fibers. The situation is somewhat different from that in the previous section, since we are effectively dealing with an eight-port device as depicted in Fig. 3, where the two channels are characterized by the transmission (T_i) and reflection (R_i) coefficients ($i=1,2$). In particular, for perfect input coupling ($R_i=0$), the system is essentially characterized by the transmission coefficients T_i.

From Eq. (10) it is easily seen that in the Fock basis a TMSV state reads

$$|\mathrm{TMSV}\rangle=\sqrt{1-|q|^2}\sum_{n=0}^{\infty}(-q)^n|n,n\rangle, \tag{25}$$

whose entanglement content is

$$E(|\mathrm{TMSV}\rangle)=-\ln(1-|q|^2)-\frac{|q|^2}{1-|q|^2}\ln|q|^2. \tag{26}$$

Application of the quantum-state transformation (14) yields ($R_i=0$) [19]

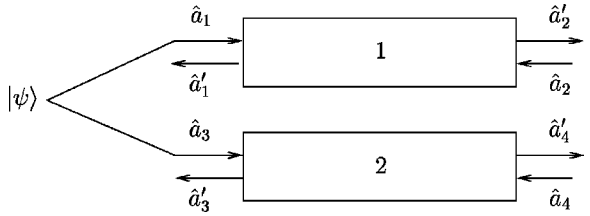

FIG. 3. A two-mode input field prepared in the quantum state $|\psi\rangle$ is transmitted through two absorbing dielectric four-port devices, $\hat{a}_1$, $\hat{a}_3$ ($\hat{a}_2'$, $\hat{a}_4'$) being the photonic operators of the relevant input (output) modes.

$$\hat{\varrho}_{\rm out}^{\rm (F)}=(1-|q|^2)\sum_{m=0}^{\infty}\sum_{k,l=0}^{\infty}[K_{k,l,m}(c_m|m+k\rangle\langle k|+\text{H.c.})\otimes(d_m|m+l\rangle\langle l|+\text{H.c.})], \tag{27}$$

where

$$c_m=(-q)^{m/2}T_1^m\left(1-\frac{1}{2}\delta_{m0}\right), \tag{28}$$

$$d_m=(-q)^{m/2}T_2^m\left(1-\frac{1}{2}\delta_{m0}\right), \tag{29}$$

and

$$K_{k,l,m}=\frac{[|q|^2(1-|T_1|^2)(1-|T_2|^2)]^a a!(a+m)!}{\sqrt{k!l!(k+m)!(l+m)!}(a-k)!(a-l)!}\left(\frac{|T_1|^2}{1-|T_1|^2}\right)^k\times\left(\frac{|T_2|^2}{1-|T_2|^2}\right)^l\times{}_2F_1\left(\begin{matrix}a+1,\ a+m+1\\ |k-l|+1\end{matrix};|q|^2(1-|T_1|^2)(1-|T_2|^2)\right) \tag{30}$$

$[a=\max(k,l)]$. Note that in Eq. (27) the fibers are assumed to be in the ground state.

A. Entanglement estimate by pure state extraction

The amount of entanglement contained in the (mixed) output state (27) can also be estimated following the line sketched in Sec. II B. In particular, the convexity of the relative entropy can be combined with Schmidt decompositions of the output state in order to calculate, on using the theorem (21), appropriate bounds on entanglement. Before doing so, let us first consider the case of low initial squeezing, for which the entanglement can be estimated rather simply.

1. Extraction of a single pure state

Since, by Eqs. (27)–(30), for low squeezing only a few matrix elements are excited that were not contained in the original Fock expansion (25), we can forget about the entanglement that could be present in the newly excited elements and treat them as contributions to the separable states only. Following [19], the inseparable state relevant for entanglement can then be estimated to be the pure state

$$\sqrt{1-\lambda}|\Psi\rangle=\sqrt{\frac{1-|q|^2}{K_{000}}}\sum_{n=0}^{\infty}K_{00n}c_nd_n|n,n\rangle. \tag{31}$$

It has the properties that only matrix elements of the same type as in the input TMSV state occur and the coefficients of the matrix elements $|0,0\rangle\leftrightarrow|n,n\rangle$ are met exactly, i.e.,

$$(1-\lambda)\langle 0,0|\Psi\rangle\langle\Psi|n,n\rangle=\langle 0,0|\hat{\varrho}_{\rm out}^{\rm (F)}|n,n\rangle. \tag{32}$$

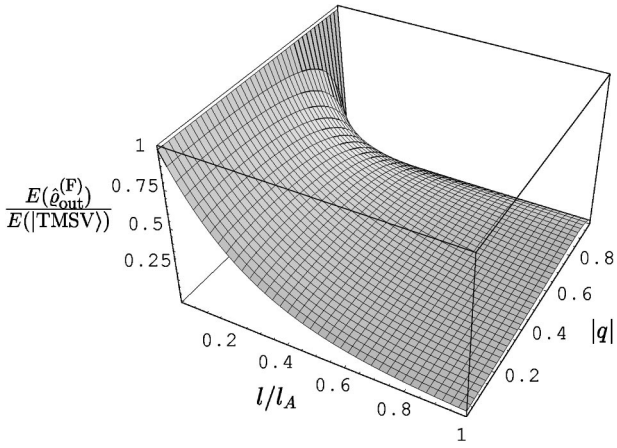

FIG. 4. Estimate of the entanglement, Eq. (33), observed after transmission of a TMSV state through absorbing fibers ($T_1=T_2$) as a function of the squeezing parameter $|q|^2$ and the transmission length l.

In this approximation, the calculation of the entanglement of the mixed output quantum state reduces to the determination of the entanglement of a pure state [19]:

$$E(\hat{\varrho}_{\rm out}^{\rm (F)})\approx(1-\lambda)E(|\Psi\rangle)=\frac{1-x}{(1-x)^2-y}\ln\left[\frac{1-x}{(1-x)^2-y}\right]+\frac{(1-x)\{[y+(1-x)^2]\ln(1-x)-y\ln y\}}{[y-(1-x)^2]^2}, \tag{33}$$

where

$$x=|q|^2(1-|T_1|^2)(1-|T_2|^2), \tag{34}$$

$$y=|qT_1T_2|^2. \tag{35}$$

Note that for $T_1=T_2=1$ the entanglement of the TMSV state is preserved, i.e., Eq. (33) reduces to Eq. (26). In Fig. 4, the estimate of entanglement as given by Eq. (33) is plotted as a function of the transmission length and the strength of initial squeezing for $T_1=T_2=T$, where T is given by the Lambert-Beer law of extinction,

$$T=e^{in_{\rm R}(\omega)\omega l/c}e^{-l/l_{\rm A}}. \tag{36}$$

Here, $n_{\rm R}$ is the real part of the complex refractive index, $l_{\rm A}=c/(n_{\rm I}\omega)$ is the absorption length, and l is the transmission length.

It is worth repeating that the estimate given by Eq. (33) is valid for low squeezing only. Higher squeezing amounts to more excited density matrix elements and Eq. (33) might become wrong. Moreover, we cannot even infer it to be a *bound* in any sense since no inequality has been involved. A possible way out would be to extract successively more and more pure states from Eq. (27). But, instead, let us turn to the Schmidt decomposition.

2. Upper bound of entanglement

In a similar way as in Sec. II B, an upper bound on the entanglement can be obtained [9] if the density operator (27) is rewritten as the convex sum of density operators in Schmidt decomposition,

$$\hat{\varrho}_{\rm out}^{(\rm F)}=\sum_{k,l=0}^{\infty}\left\{A_{k,l}|k,k\rangle\langle l,l|+\sum_{m=1}^{\infty}B_{k,l,m}|k+m,k\rangle \otimes\langle l+m,l|+\sum_{m=1}^{\infty}C_{k,l,m}|k,k+m\rangle\langle l,l+m|\right\}, \tag{37}$$

and the inequality (22) together with Eq. (21) is applied.

From general arguments one would expect the entanglement to decrease faster the more squeezing one puts into the TMSV, because stronger squeezing is equivalent to saying the state is more macroscopically nonclassical and quantum correlations should be destroyed faster. As an example, one would have to look at the entanglement degradation of an n-photon Bell-type state $|\Psi_n^{\pm}\rangle$, $E(|\Psi_n^{\pm}\rangle)\leqslant|T|^{2n}\ln 2$ [25]. Since the transmission coefficient T decreases exponentially with increasing transmission length, entanglement decreases even faster. Note that similar arguments also hold for the destruction of the interference pattern of a catlike state $\sim|\alpha\rangle+|-\alpha\rangle$ when it is transmitted, e.g., through a beam splitter. It is well known that the two peaks (in the jth output channel) decay as $|T_{j1}|^2$, whereas the quantum interference decays as $|T_{j1}|^2\exp[-2|\alpha|^2(1-|T_{j1}|^2)]$.

The upper bound on the entanglement as calculated above seems to suggest that the entanglement degradation is simply exponential with the transmission length for essentially all (initial) squeezing parameters, which would make the TMSV a good candidate for a robust entangled quantum state. But this is a fallacy. The higher the squeezing, the more density matrix elements are excited, and the more terms appear, according to Eq. (37), in the convex sum (22). Equivalently, more and more separable states are mixed into the full quantum state. Thus the inequality gets more inadequate. In order to see this, we have shown in Fig. 5 the upper bound on the entanglement for just two different (initial) squeezing parameters $|q|=0.71$ (equivalent to the mean photon number of $\overline{n}=1$, solid line) and $|q|=0.9535$ ($\overline{n}=10$, dashed line). For small transmission lengths, where very few separable states are mixed in, the curves show the expected behavior in the sense that the state with higher initial squeezing decoheres fastest. The behavior changes for larger transmission lengths. We would thus conclude that the upper bound proposed in [9] is insufficient.

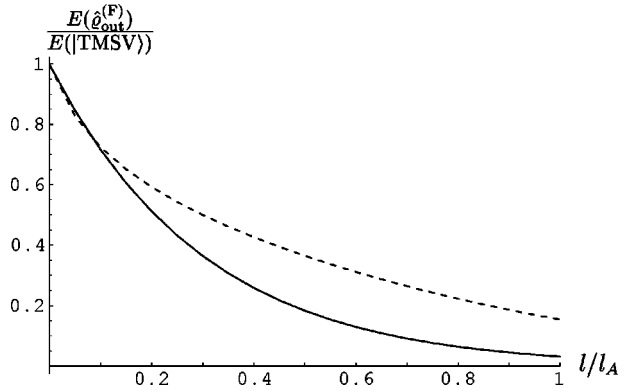

FIG. 5. Upper bound of the entanglement degradation of a TMSV state transmitted through absorbing fibers ($T_1=T_2$) as a function of the transmission length l for the squeezing parameters $q=0.1$ (solid line) and $q=0.9$ (dashed line). In the numerical calculation, Fock states $|n\rangle$ up to $q^n\leqslant 0.02$ have been taken into account.

B. Distance to separable Gaussian states

The methods of computing entanglement estimates and bounds as considered in the preceding sections are based on Fock-state expansions. In practice they are typically restricted to situations where only a few quanta of the overall system (consisting of the field and the device) are excited, otherwise the calculation even of the matrix elements becomes arduous. Here we will focus on another way of computing the relative entropy, which will also enable us to give an essentially better bound on the entanglement (for other quantities that in a sense characterize entanglement, see [26]).

Since it is close to impossible to compute the distance of a Gaussian state to the set of *all* separable states we restrict ourselves to separable *Gaussian* states. A quantum state is commonly called Gaussian if its quantum characteristic function is Gaussian. By the general relation for an N-mode quantum state

$$\hat{\sigma}=\frac{1}{\pi^N}\int d^{2N}\boldsymbol{\alpha}\,\chi(-\boldsymbol{\alpha})\hat{D}(\boldsymbol{\alpha}) \tag{38}$$

it is obvious that the density operator of a Gaussian state can be written in exponential form as

$$\hat{\sigma}=\mathcal{N}\exp\left[-(\hat{a}^\dagger\hat{a})\mathbf{M}_\sigma\begin{pmatrix}\hat{a}\\ \hat{a}^\dagger\end{pmatrix}\right], \tag{39}$$

where $\mathbf{M}_\sigma$ is a Hermitian matrix that can be assumed to give a symmetrically ordered density operator, and $\mathcal{N}$ is a suitable normalization factor. Here and in the following we restrict ourselves to Gaussian states with zero mean. Since coherent displacements, being local unitary transformations, do not influence entanglement, they can be disregarded.

The relative entropy (19) can now be written as

$$\begin{aligned}E_R(\hat{\varrho})&=\min_{\hat{\sigma}\in\mathcal{S}}{\rm Tr}\left\{\hat{\varrho}\left[\ln\hat{\varrho}-\ln\mathcal{N}+(\hat{a}^\dagger\hat{a})\mathbf{M}_\sigma\begin{pmatrix}\hat{a}\\ \hat{a}^\dagger\end{pmatrix}\right]\right\}\\ &={\rm Tr}(\hat{\varrho}\ln\hat{\varrho})+\min_{\hat{\sigma}\in\mathcal{S}}\left\langle(\hat{a}^\dagger\hat{a})\mathbf{M}_\sigma\begin{pmatrix}\hat{a}\\ \hat{a}^\dagger\end{pmatrix}-\ln\mathcal{N}\right\rangle_{\hat{\varrho}}.\end{aligned} \tag{40}$$

Since we have chosen the density operator $\hat{\sigma}$ to be symmetrically ordered, the last term in Eq. (40) is nothing but a sum

of (weighted) symmetrically ordered expectation values $\langle \hat{a}^{\dagger m}\hat{a}^{n}\rangle_{s=0}$ $(m+n=2)$. For a Gaussian quantum state $\hat{\varrho}$ it can be shown (Appendix B) that Eq. (40) can equivalently be written in terms of the matrix $\mathbf{D}_{\varrho}$ in the exponential of the characteristic function of $\hat{\varrho}$ as

$$E_R(\hat{\varrho}) = \mathrm{Tr}(\hat{\varrho}\ln\hat{\varrho}) + \min_{\hat{\sigma}\in\mathcal{S}}\left[\frac{1}{2}\mathrm{Tr}(\mathbf{M}_{\sigma}\mathbf{D}_{\varrho}) - \ln\mathcal{N}\right]. \quad (41)$$

From the above it is clear that we need only the matrix $\mathbf{D}_{\varrho}$ (which is unitarily equivalent to the variance matrix). For a Gaussian distribution with zero mean the elements of the variance matrix $\mathbf{V}$ are defined by $V_{ij}=\langle \hat{\zeta}_i,\hat{\zeta}_j\rangle_{s=0}$ as the (symmetrically ordered) expectation values of the quadrature components $\hat{\boldsymbol{\zeta}}=(\hat{x}_1,\hat{p}_1,\hat{x}_2,\hat{p}_2)$.

The variance matrix of the TMSV state (25) reads ($q=\tanh|\xi|e^{i\phi}$, $\xi=|\xi|e^{i\phi}$)

$$\mathbf{V}_{\varrho}=\begin{pmatrix}\mathbf{X} & \mathbf{Z}\\ \mathbf{Z}^{\mathrm{T}} & \mathbf{Y}\end{pmatrix}=\begin{pmatrix} c/2 & 0 & -s_1/2 & -s_2/2\\ 0 & c/2 & -s_2/2 & s_1/2\\ -s_1/2 & -s_2/2 & c/2 & 0\\ -s_2/2 & s_1/2 & 0 & c/2\end{pmatrix}, \quad (42)$$

with the notation $c=\cosh 2|\xi|$, $s_1=\sinh 2|\xi|\cos\phi$, and $s_2=\sinh 2|\xi|\sin\phi$. In the case $\phi=0$ the variance matrix (42) reduces to the generic form

$$\mathbf{V}_0=\begin{pmatrix} x & 0 & z_1 & 0\\ 0 & x & 0 & z_2\\ z_1 & 0 & y & 0\\ 0 & z_2 & 0 & y\end{pmatrix} \quad (43)$$

specified by four real parameters. Note that the variance matrix of any Gaussian state can be brought to the form (43) by local $\mathrm{Sp}(2,\mathbb{R})\otimes\mathrm{Sp}(2,\mathbb{R})$ transformations [27], so that we can restrict further discussion to that case.

Application of the input-output relations (13) gives for the elements of the variance matrix of the output state [19], on assuming that the two modes are transmitted through two four-port devices prepared in thermal states of mean photon numbers $n_{\mathrm{th}i}$,

$$X_{11}=X_{22}=\frac{1}{2}c|T_1|^2+\frac{1}{2}|R_1|^2+\left(n_{\mathrm{th}1}+\frac{1}{2}\right)(1-|T_1|^2-|R_1|^2), \quad (44)$$

$$Y_{11}=Y_{22}=\frac{1}{2}c|T_2|^2+\frac{1}{2}|R_2|^2+\left(n_{\mathrm{th}2}+\frac{1}{2}\right)(1-|T_2|^2-|R_2|^2), \quad (45)$$

$$Z_{11}=-Z_{22}=-\frac{1}{2}s\,\mathrm{Re}(T_1T_2), \quad (46)$$

$$Z_{12}=Z_{21}=-\frac{1}{2}s\,\mathrm{Im}(T_1T_2) \quad (47)$$

($\phi=0$, $s=\sinh 2|\xi|$). With regard to optical fibers with perfect input coupling ($R_i=0$) and equal transmission lengths, we again may set $|T_i|=e^{-l/l_{\mathrm{A}}}$. Moreover, we may assume real T_i and thus set $Z_{12}=Z_{21}=0$.

First, one can check for separability according to the criterion [27,28]

$$\det\mathbf{X}\det\mathbf{Y}+\left(\frac{1}{4}-|\det\mathbf{Z}|\right)^2-\mathrm{Tr}(\mathbf{XJZJYJZ}^{\mathrm{T}}\mathbf{J}) \geqslant \frac{1}{4}(\det\mathbf{X}+\det\mathbf{Y}), \quad (48)$$

which reduces to

$$4(xy-z_1^2)(xy-z_2^2)\geqslant(x^2+y^2)+2|z_1z_2|-\frac{1}{4}. \quad (49)$$

Combining Eqs. (44)–(49), it is not difficult to prove that the boundary between separability and inseparability is reached for [19,28,29]

$$l=l_{\mathrm{S}}\equiv\frac{l_{\mathrm{A}}}{2}\ln\left[1+\frac{1}{n_{\mathrm{th}}}(1-e^{-2|\xi|})\right]. \quad (50)$$

It is worth noting that this is exactly the same condition as for the transmitted state still being a squeezed state or not. To show this, we calculate the normally ordered variance $\langle{:}(\Delta\hat{F})^2{:}\rangle$ of a phase-sensitive quantity such as $\hat{F}=|F_1|e^{i\varphi_1}\hat{a}_1+|F_2|e^{i\varphi_2}\hat{a}_2+\mathrm{H.c.}$ Using the input-output relations (13), the normally ordered variance of the output field is derived to be

$$\begin{aligned}\langle{:}(\Delta\hat{F})^2{:}\rangle_{\mathrm{out}} &= 2|F_1|^2[|T_1|^2\sinh^2|\xi|+n_{\mathrm{th}1}(1-|T_1|^2)]\\ &\quad+2|F_2|^2[|T_2|^2\sinh^2|\xi|+n_{\mathrm{th}2}(1-|T_2|^2)]\\ &\quad-2|F_1F_2T_1T_2|\sinh 2|\xi|\cos(\varphi_1+\varphi_2+\varphi_T+\phi)\end{aligned} \quad (51)$$

($T_i=|T_i|e^{i\varphi_{T_i}}$, $i=1,2$; $\varphi_T=\varphi_{T_1}+\varphi_{T_2}$). For equal amplitudes $|F_1|=|F_2|=|F|$ and equal fibers $|T_1|=|T_2|=|T|$, $n_{\mathrm{th}1}=n_{\mathrm{th}2}=n_{\mathrm{th}}$ the (phase-dependent) minimum is obtained as

$$\langle{:}(\Delta\hat{F})^2{:}\rangle_{\mathrm{out}}|_{\min}=4|F|^2[n_{\mathrm{th}}(1-|T|^2)-|T|^2\sinh|\xi|e^{-|\xi|}]. \quad (52)$$

Equation (52) exactly leads to the condition (50), i.e.,

$$\langle{:}(\Delta\hat{F})^2{:}\rangle_{\mathrm{out}}|_{\min}\begin{cases}<0 & \text{if}\quad l<l_{\mathrm{S}},\\ \geqslant 0 & \text{if}\quad l\geqslant l_{\mathrm{S}}.\end{cases} \quad (53)$$

Therefore, measurement of squeezing corresponds, in some sense, to an entanglement measurement.

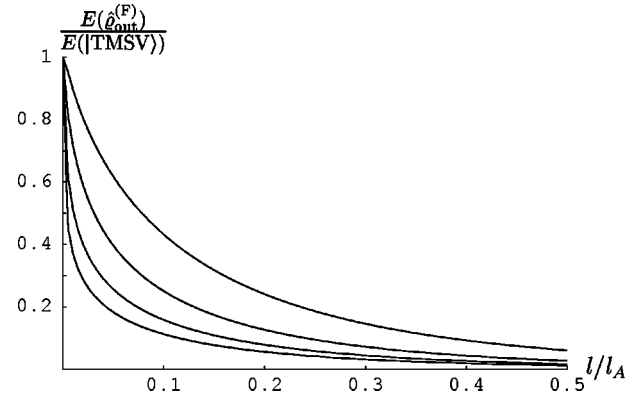

FIG. 6. Entanglement degradation of a TMSV state transmitted through absorbing fibers ($T_1=T_2$) as a function of the transmission length l for the (initial) mean photon numbers $\bar{n}=1$ ($|q|\approx 0.7071$) (topmost curve), $\bar{n}=10$ ($|q|\approx 0.9535$), $\bar{n}=10^2$ ($|q|\approx 0.9950$), and $\bar{n}=10^3$ ($|q|\approx 0.9995$) (lowest curve).

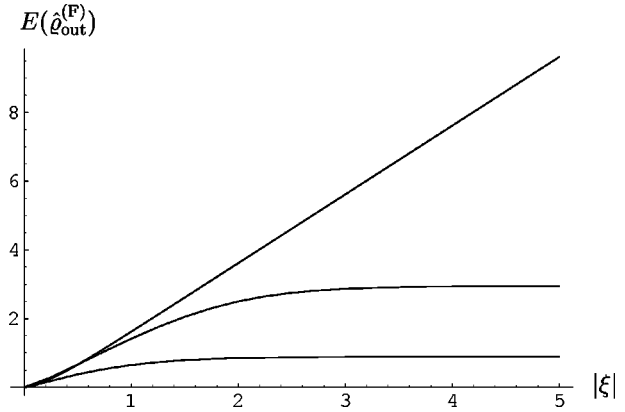

FIG. 7. Available entanglement after transmission of a TMSV state through absorbing fibers ($T_1=T_2$) as a function of the squeezing parameter ξ for various transmission lengths l [$l=0$ (topmost curve), $l=10^{-2}l_A$ (middle curve), $l=10^{-1}l_A$ (lowest curve)]. For $|\xi|\lesssim 0.5$ and $l/l_A\lesssim 10^{-2}$, the numerical accuracy of the values of $E(\hat{\varrho}_{\rm out}^{(\rm F)})$ decreases due to low accuracy in the eigenvector computation.

In order to obtain (for $l<l_{\rm S}$) a measure of the entanglement degradation, we compute the distance of the output quantum state to the set of all Gaussian states satisfying the *equality* in (49), since they just represent the boundary between separability and inseparability. These states are completely specified by only three real parameters [one of the parameters in the equality in (49) can be computed from the other three]. With regard to Eq. (41), minimization is thus performed only in a three-dimensional parameter space. Results of our numerical analysis are shown in Fig. 6. It is clearly seen that the entanglement content (relative to the entanglement in the initial TMSV state) decreases noticeably faster for larger squeezing, or, equivalently, for higher mean photon number [the relation between the mean photon number $\bar{n}$ in one mode and the squeezing parameters being $\bar{n}=\sinh^2|\xi|=|q|^2/(1-|q|^2)$].

It is very instructive to know how much entanglement is available after transmission of the TMSV state through the fibers. Examples of the (maximally) available entanglement for different transmission lengths are shown in Fig. 7. One observes that a chosen transmission length allows only for transport of a certain amount of entanglement. The saturation value, which is quite independent of the value of the input entanglement, decreases drastically with increasing transmission length (compare the upper curve with the two lower curves in the figure).

The reason for the saturation effect is rather general and not restricted to the TMSV state under study. The quantum-state transformation (14) corresponds to a convolution of the phase-space functions of the incoming field and the device noise [18], the latter being responsible for entanglement degradation. Eventually, the width of the noise Gaussian prevents recovery, after transmission, of the phase-space structure that is typical of a (strongly) entangled state. For example, an infinitely squeezed TMSV state gives rise to infinitely narrow Wigner functions along certain directions in the phase space. Thus, after transmission finite widths are observed which are solely determined by the noise of the device.

Obviously, saturation of entanglement has dramatic consequences for applications in quantum information processing. For example, in continuous-variable teleportation a highly squeezed TMSV state is required in order to teleport an arbitrary quantum state with sufficiently high fidelity [2]. Even if the input TMSV state were infinitely squeezed, the available (low) saturation value of entanglement prevents one from high-fidelity teleportation of *arbitrary* quantum states over finite distances [29–32].

A very illustrative example is quantum dense coding where a classical bit is encoded in a coherent shift $\hat{D}(\pm\alpha)$ of one mode of a TMSV state. The analysis given in [6] shows that, when the state is subject to decoherence during transmission through a symmetric channel, then quantum dense coding is superior to classical coding only if, in the strong-squeezing limit, the transmission coefficient does not drop below $|T|^2=0.75$. Looking at Fig. 7 and noting that this value of the transmission coefficient corresponds to a fiber length of $l\approx 0.14 l_{\rm A}$, one realizes that the maximal possible amount of entanglement that can be transmitted through such fibers is roughly $E\approx 0.7$. But this is precisely the amount of (quantum) information needed to transmit one bit of (classical) information encoded in an infinitely squeezed input TMSV state. That means that it is impossible to transmit the information even of a single classical bit quantum mechanically over distances longer than $l\approx 0.14 l_{\rm A}$, thereby rendering this type of quantum information processing useless.

C. Comparison of the methods

In Fig. 8 the entanglement degradation as calculated in Sec. III B is compared with the estimate obtained in Sec. III A 1 and the bound obtained in Sec. III A 2. The figure reveals that the distance of the output state to the separable Gaussian states (lower curve) is much smaller than might be expected from the bound on the entanglement (upper curve) calculated according to Eq. (24) together with Eqs. (21) and

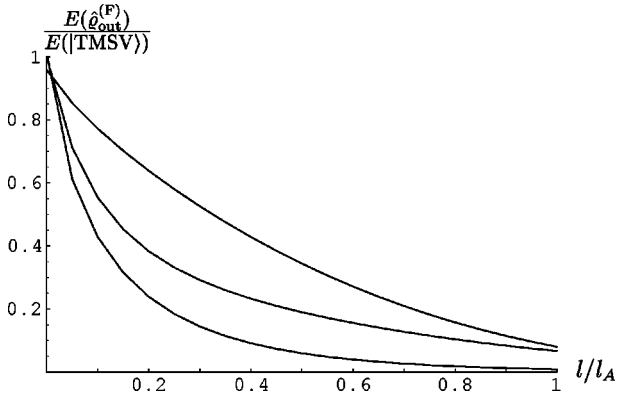

FIG. 8. Comparison of the upper bound on entanglement (upper curve) according to Eq. (37), the entanglement estimate (middle curve) according to Eq. (33), and the distance measure (lower curve) according to Eq. (41) for the mean photon number $\bar{n}=1$ ($|q|\simeq 0.7071$).

(37), as well as the estimate (middle curve) derived by extracting a single pure state according to Eq. (33). Note that the entanglement of the single pure state (31) comes closest to the distance of the actual state to the separable Gaussian states, whereas the convex sum (37) of density operators in Schmidt decomposition can give much higher values. Both methods, however, overestimate the entanglement. Since with increasing mean photon number the convex sum contains more and more terms, the bound gets worse [and substantially slower on the computer, whereas computation of the distance measure (41) does not depend on it].

Thus, in our view, the distance to the separable Gaussian states should be the measure of choice for determining the entanglement degradation of entangled Gaussian states. Nevertheless, it should be pointed out that the distance to separable Gaussian states has been considered, and not the distance to all separable states. We have no proof yet that there does not exist an inseparable non-Gaussian state that is closer than the closest Gaussian state.

IV. CONCLUSIONS

In the present article the interferometric generation and transmission of entangled light have been studied, with special emphasis on Gaussian states. Optical devices such as beam splitters and fibers are regarded as being dispersing and absorbing dielectric four-port devices as typically used in practice. In particular, their action on light is described in terms of the experimentally measurable transmission, reflection, and absorption coefficients.

An entangled two-mode state can be generated by mixing single-mode nonclassical light at a beam splitter. Depending on the phases of the impinging light beams and the beam splitter transformation, the amount of entanglement contained in the outgoing light can be controlled. For squeezed vacuum input states and appropriately chosen phases, maximal entanglement is obtained for lossless, symmetrical beam splitters. In realistic experiments, however, losses such as material absorption prevent one from realizing that value.

When entangled light is transmitted through optical devices, losses always give rise to entanglement degradation. In particular, after propagation of the two modes of a two-mode squeezed vacuum through fibers the available entanglement can be drastically reduced. Unfortunately, quantifying the entanglement of mixed states in an infinite-dimensional Hilbert spaces has been close to impossible. Therefore, estimates and upper bounds for the entanglement content have been developed.

The analytical estimate employed in this article is based on extraction of a single pure state from the output Gaussian state, using its reduced von Neumann entropy as an estimate for the entanglement. However, this method is not unique, since there are many different ways of extracting pure states, nor is it an upper bound, since nothing is said about the residual entanglement contained in the state that is left over. In principle, more and more pure states could be extracted until the residual state becomes separable.

Instead, an upper bound can be calculated by decomposing the output Gaussian state into a convex sum of Schmidt states as proposed in [9]. The disadvantage of this method is that the bound gets worse for increasing (statistical) mixing. In particular, it may give hints of large entanglement even if the quantum state under consideration is almost separable.

In order to overcome this disadvantage, the distance of the output Gaussian state to the set of separable Gaussian states measured by the relative entropy is considered. It has the advantage that separable states obviously correspond to zero distance. Although one has yet no proof that there does not exist a non-Gaussian separable state that is closer to the Gaussian state under consideration than the closest separable Gaussian state, one has good reason to think that it is even an entanglement measure. In any case, it is a much better bound than the one obtained by convexity. In particular, it clearly demonstrates the drastic decrease of entanglement of the output state with increasing entanglement of the input state. Moreover, one observes saturation of entanglement transfer; that is, the amount of entanglement that can maximally be contained in the output state is solely determined by the transmission length and does not depend on the amount of entanglement contained in the input state.

ACKNOWLEDGMENTS

S.S. wishes to thank V. I. Man'ko for helpful discussions on multivariable Hermite polynomials. The authors also acknowledge discussions about Gaussian quantum states with E. Schmidt.

APPENDIX A: FOCK-STATE EXPANSION OF MULTIMODE SQUEEZED VACUUM STATES

Let us consider an incoming field prepared in the squeezed vacuum state (4) and an absorbing beam splitter in the ground state. The quantum-state transformation formula (14) then leads to

$$\hat{\varrho}_{\rm out}^{(\rm F)}=\sum_{g_1,g_2=0}^{\infty}\langle g_1,g_2|\hat{S}_{a_1'}(\xi_1)\hat{S}_{a_2'}(\xi_2)|0,0,0,0\rangle \otimes\langle 0,0,0,0|\hat{S}_{a_2'}^{\dagger}(\xi_2)\hat{S}_{a_1'}^{\dagger}(\xi_1)|g_1,g_2\rangle \tag{A1}$$

where the transformed operators $\hat{a}_i'$ are defined by

$$\hat{a}_i' = \sum_{j=1}^{4} \Lambda_{ji}^{*} \hat{a}_j \tag{A2}$$

according to the rules of quantum-state transformation. Equivalently, the Fock-state expansion of the density matrix reads

$$\begin{aligned}\langle m_1,m_2|\hat{\varrho}_{\rm out}^{(\rm F)}|n_1,n_2\rangle &= \langle m_1,m_2|\langle g_1,g_2|\hat{S}_{a_1'}(\xi_1)\hat{S}_{a_2'}(\xi_2)|0,0,0,0\rangle \\ &\otimes\langle 0,0,0,0|\hat{S}_{a_2'}^{\dagger}(\xi_2)\hat{S}_{a_1'}^{\dagger}(\xi_1)|g_1,g_2\rangle|n_1,n_2\rangle. \end{aligned}\tag{A3}$$

Expanding the Fock states in terms of coherent states and using the squeeze operator in the form given in the second equality in Eq. (5), we obtain after performing all integrals

$$\begin{aligned}\langle m_1,m_2|\hat{\varrho}_{\rm out}^{(\rm F)}|n_1,n_2\rangle &= \sqrt{\frac{(1-|q_1|^2)(1-|q_2|^2)}{m_1!m_2!n_1!n_2!}}(-1)^{m_1+m_2+n_1+n_2} \\ &\times\sum_{g_1,g_2=0}^{\infty}\frac{1}{g_1!g_2!}H_{m_1,m_2,g_1,g_2}^{\mathbf{M}}(\mathbf{0})H_{n_1,n_2,g_1,g_2}^{*\mathbf{M}}(\mathbf{0}),\end{aligned}\tag{A4}$$

where the Hermite polynomials of four variables are generated by the symmetric matrix $\mathbf{M}$ with elements

$$M_{ij} = q_1\Lambda_{i1}\Lambda_{j1} + q_2\Lambda_{i2}\Lambda_{j2}. \tag{A5}$$

Using the relation between Hermite polynomials of one variable and those of several variables [33],

$$\begin{aligned}\sum_{m_1+\cdots+m_n=m}\frac{a_1^{m_1}}{m_1!}\cdots\frac{a_n^{m_n}}{m_n!}H_{m_1,\ldots,m_n}^{\mathbf{M}}(x_1,\ldots,x_n) &= \frac{\left[\frac{1}{2}\phi(\mathbf{a})\right]^{m/2}}{m!}H_m\left(\frac{\phi(\mathbf{a},\mathbf{x})}{\sqrt{2\phi(\mathbf{a})}}\right),\end{aligned}\tag{A6}$$

where

$$\phi(\mathbf{a},\mathbf{x}) = \sum_{i,j} a_i M_{ij} x_j \tag{A7}$$

and $\phi(\mathbf{a})\equiv\phi(\mathbf{a},\mathbf{a})$, we get for the multivariable Hermite polynomial of zero argument

$$\begin{aligned}H_{m_1,m_2,g_1,g_2}^{\mathbf{M}}(\mathbf{0}) &= \frac{H_m(0)}{2^{m/2}}\frac{m_1!m_2!g_1!g_2!}{m!} \\ &\times\sum_{\mathcal{P}}\underbrace{M_{i_1,j_1}M_{i_2,j_2}\cdots M_{i_{m/2},j_{m/2}}}_{m/2\text{ terms}}\end{aligned}\tag{A8}$$

$(m=m_1+m_2+g_1+g_2)$. Here, the $\mathcal{P}$ sum runs over all $m!/(m_1!m_2!g_1!g_2!)$ possible combinations to distribute m_1 indices 1, m_2 indices 2, g_1 indices 3, and g_2 indices 4 among the indices $i_1,j_1,\ldots,i_{m/2},j_{m/2}$.

In particular, if we restrict ourselves to two dimensions, Eq. (A8) simplifies to

$$\begin{aligned}H_{m_1,m_2}^{\mathbf{M}}(\mathbf{0}) &= \frac{H_m(0)}{2^{m/2}}M_{11}^{(m_1-m_2-\nu)/4}M_{22}^{(m_2-m_1-\nu)/4}m_1!m_2!\left(\frac{m}{2}\right)! \\ &\times\sum_{n=\nu/2}^{[\mu/2]}\frac{1}{n!(\mu-2n)!\left(n-\frac{1}{2}\nu\right)!}M_{11}^{n}(2M_{12})^{\mu-2n}M_{22}^{n}\end{aligned}\tag{A9}$$

$[\mu=\max(m_1,m_2),\nu=|m_1-m_2|]$. The sum can also be calculated, leading to Gegenbauer, Jacobi, or associated Legendre polynomials [34].

Another way of writing this is the one we used for the numerical calculation of the density matrix elements. The method, however, is applicable only in cases where the number of variables the Hermite polynomial depends on is sufficiently small. The multivariable Hermite polynomial (now in four variables) of zero argument can be written as

$$\begin{aligned}(-1)^{m_1+m_2+g_1+g_2}H_{m_1,m_2,g_1,g_2}^{\mathbf{M}}(\mathbf{0}) &= \frac{\partial^{m_1+m_2+g_1+g_2}}{\partial\lambda_1^{m_1}\partial\lambda_2^{m_2}\partial\lambda_3^{g_1}\partial\lambda_4^{g_2}}\exp\left[-\frac{1}{2}\boldsymbol{\lambda}^{\rm T}\mathbf{M}\boldsymbol{\lambda}\right]_{\boldsymbol{\lambda}=\mathbf{0}},\end{aligned}\tag{A10}$$

with $\mathbf{M}$ being given by Eq. (A5). Expanding the right hand side of Eq. (A10), the only surviving term is the one proportional to $(\boldsymbol{\lambda}^{\rm T}\mathbf{M}\boldsymbol{\lambda})^{(m_1+m_2+g_1+g_2)/2}$. Multinomial expansion of this term then leads to Eq. (17).

APPENDIX B: MULTIMODE GAUSSIAN DENSITY OPERATORS AND WIGNER FUNCTIONS

We start with the Wigner function of an N-mode Gaussian state of the form as

$$W_N(\boldsymbol{\zeta}) = \frac{1}{(2\pi)^N\sqrt{\det\mathbf{V}}}\exp\left(-\frac{1}{2}\boldsymbol{\zeta}^{\rm T}\mathbf{V}^{-1}\boldsymbol{\zeta}\right), \tag{B1}$$

where $\boldsymbol{\zeta}=(x_1,p_1,\ldots,x_N,p_N)$ is the $2N$-dimensional "vector" of the quadrature components of the N (complex) variables $\hat{a}_i$ and $\mathbf{V}$ is the $2N\times 2N$ variance matrix of the quadrature components. The characteristic function defined by the Fourier transform reads

$$\chi_N(\boldsymbol{\eta})=\exp\left(-\frac{1}{2}\boldsymbol{\eta}^{\mathrm{T}}\mathbf{V}\boldsymbol{\eta}\right). \tag{B2}$$

Alternatively, the quantum state can be given by the density operator

$$\hat{\varrho}=\frac{\exp\left[-\frac{1}{2}(\hat{a}^\dagger\hat{a})\mathbf{M}\begin{pmatrix}\hat{a}\\ \hat{a}^\dagger\end{pmatrix}\right]}{\mathrm{Tr}\left\{\exp\left[-(\hat{a}^\dagger\hat{a})\mathbf{M}\begin{pmatrix}\hat{a}\\ \hat{a}^\dagger\end{pmatrix}\right]\right\}} \tag{B3}$$

(where $\hat{a}$ is actually an N-dimensional "vector" with "components" $\hat{a}_i$).

In order to relate the matrix $\mathbf{M}$ to the matrix $\mathbf{V}$, we introduce a unitary transformation

$$\begin{pmatrix}\hat{a}\\ \hat{a}^\dagger\end{pmatrix}'=\hat{U}\begin{pmatrix}\hat{a}\\ \hat{a}^\dagger\end{pmatrix}\hat{U}^{-1}=\mathbf{U}\begin{pmatrix}\hat{a}\\ \hat{a}^\dagger\end{pmatrix}, \tag{B4}$$

where the matrix $\mathbf{U}$ is chosen such that it diagonalizes $\mathbf{M}$; hence $\mathbf{U}^+\mathbf{M}\mathbf{U}=\boldsymbol{\Theta}$ (with $\boldsymbol{\Theta}$ being diagonal). Note that $\mathbf{U}$ satisfies the generalized unitary relation

$$\mathbf{U}\mathbf{J}\mathbf{U}^+=\mathbf{J} \quad \text{with} \quad \mathbf{J}=\mathrm{diag}(\mathbf{I}_N,-\mathbf{I}_N). \tag{B5}$$

Then, the characteristic function of the density operator (B2) is

$$\begin{aligned}\chi_N(\boldsymbol{\lambda},\boldsymbol{\lambda}^*)&=\mathrm{Tr}[\hat{\varrho}\hat{D}(\boldsymbol{\lambda})]=\mathrm{Tr}\left\{\hat{\varrho}\exp\left[(\hat{a}^\dagger\hat{a})\begin{pmatrix}\boldsymbol{\lambda}\\ -\boldsymbol{\lambda}^*\end{pmatrix}\right]\right\}\\ &=\mathrm{Tr}\left\{\hat{U}\hat{\varrho}\hat{U}^{-1}\hat{U}\exp\left[(\hat{a}^\dagger\hat{a})\begin{pmatrix}\boldsymbol{\lambda}\\ -\boldsymbol{\lambda}^*\end{pmatrix}\right]\hat{U}^{-1}\right\}\\ &=\exp\left[-\frac{1}{2}\begin{pmatrix}\boldsymbol{\lambda}\\ -\boldsymbol{\lambda}^*\end{pmatrix}^+\mathbf{U}\left(\frac{1}{2}\coth\frac{1}{2}\boldsymbol{\Theta}\right)\mathbf{U}^+\begin{pmatrix}\boldsymbol{\lambda}\\ -\boldsymbol{\lambda}^*\end{pmatrix}\right]\\ &=\exp\left[-\frac{1}{2}\begin{pmatrix}\boldsymbol{\lambda}\\ \boldsymbol{\lambda}^*\end{pmatrix}^+\mathbf{D}\begin{pmatrix}\boldsymbol{\lambda}\\ \boldsymbol{\lambda}^*\end{pmatrix}\right]\end{aligned} \tag{B6}$$

with an obvious definition of the matrix $\mathbf{D}$, thus establishing a relation between the matrix $\mathbf{M}$ in the exponential of the density operator and the matrix $\mathbf{D}$ in the exponential of the characteristic function. From the third to the fourth equality in Eq. (B6) we have used the expression for the characteristic function of a thermal state [35]. In due course, the normalization of the density operator is obtained as

$$\mathcal{N}=\prod_{i=1}^{N}2\sinh\frac{\Theta_i}{2}. \tag{B7}$$

The above description shows a way to compute the entropy of a Gaussian quantum state $\hat{\varrho}$ as well as the relative entropy between two Gaussian quantum states $\hat{\varrho}$ and $\hat{\sigma}$ as

$$\mathrm{Tr}(\hat{\varrho}\ln\hat{\varrho})=\sum_{i=1}^{N}\ln\left(2\sinh\frac{\Theta_i}{2}\right)-\frac{1}{2}\mathrm{Tr}(\mathbf{M}_\varrho\mathbf{D}_\varrho), \tag{B8}$$

$$\mathrm{Tr}(\hat{\varrho}\ln\hat{\sigma})=\sum_{i=1}^{N}\ln\left(2\sinh\frac{\vartheta_i}{2}\right)-\frac{1}{2}\mathrm{Tr}(\mathbf{M}_\sigma\mathbf{D}_\varrho), \tag{B9}$$

where Θ_i and ϑ_i are, respectively, the eigenvalues of $\mathbf{M}_\varrho$ and $\mathbf{M}_\sigma$.

[1] N. Korolkova and G. Leuchs, in *Coherence and Statistics of Photons and Atoms*, edited by J. Peřina (Wiley, New York, 2001).

[2] S. L. Braunstein and H. J. Kimble, Phys. Rev. Lett. **80**, 869 (1998).

[3] A. Furusawa, J. L. Sorensen, S. L. Braunstein, C. A. Fuchs, H. J. Kimble, and E. S. Polzik, Science **282**, 706 (1998).

[4] G. J. Milburn and S. L. Braunstein, Phys. Rev. A **60**, 937 (1999).

[5] M. Ban, J. Opt. B: Quantum Semiclassical Opt. **1**, L9 (1999).

[6] M. Ban, J. Opt. B: Quantum Semiclassical Opt. **2**, 786 (2000).

[7] S. L. Braunstein and H. J. Kimble, Phys. Rev. A **61**, 042302 (2000).

[8] V. Vedral and M. B. Plenio, Phys. Rev. A **57**, 1619 (1998).

[9] T. Hiroshima, Phys. Rev. A **63**, 022305 (2001).

[10] B. Yurke, S. L. McCall, and J. R. Klauder, Phys. Rev. A **33**, 4033 (1986).

[11] S. Prasad, M. O. Scully, and W. Martienssen, Opt. Commun. **62**, 139 (1987).

[12] Z. Y. Ou, C. K. Hong, and L. Mandel, Opt. Commun. **63**, 118 (1987).

[13] H. Fearn and R. Loudon, Opt. Commun. **64**, 485 (1987).

[14] M. A. Campos, B. E. A. Saleh, and M. C. Teich, Phys. Rev. A **40**, 1371 (1989).

[15] U. Leonhardt, Phys. Rev. A **48**, 3265 (1993).

[16] K. Wódkiewicz and J. H. Eberly, J. Opt. Soc. Am. B **2**, 458 (1985).

[17] X. Ma and W. Rhodes, Phys. Rev. A **41**, 4625 (1990).

[18] L. Knöll, S. Scheel, E. Schmidt, D.-G. Welsch, and A. V. Chizhov, Phys. Rev. A **60**, 4716 (1999).

[19] S. Scheel, T. Opatrný, and D.-G. Welsch, Opt. Spectrosc. **97**, 447 (2001).

[20] L. Knöll, S. Scheel, and D.-G. Welsch, in *Coherence and Statistics of Photons and Atoms* (Ref. [1]).

[21] S. Parker, S. Bose, and M. B. Plenio, Phys. Rev. A **61**, 032305 (2000).

[22] E. M. Rains, Phys. Rev. A **60**, 179 (1999).

[23] S. Wu and Y. Zhang, Phys. Rev. A **63**, 012308 (2001).

[24] T. Gruner and D.-G. Welsch, Phys. Rev. A **54**, 1661 (1996).
[25] S. Scheel, L. Knöll, T. Opatrný, and D.-G. Welsch, Phys. Rev. A **62**, 043803 (2000).
[26] A. V. Chizhov, E. Schmidt, L. Knöll, and D.-G. Welsch, J. Opt. B: Quantum Semiclassical Opt. **3**, 1 (2001).
[27] R. Simon, Phys. Rev. Lett. **84**, 2726 (2000).
[28] L.-M. Duan, G. Giedke, J. I. Cirac, and P. Zoller, Phys. Rev. Lett. **84**, 2722 (2000).
[29] J. Lee, M. S. Kim, and H. Jeong, Phys. Rev. A **62**, 032305 (2000).
[30] M. S. Kim and J. Lee, Phys. Rev. A **64**, 012309 (2001).
[31] M. S. Kim and J. Lee, Phys. Rev. A **64**, 012309 (2001).
[32] D.-G. Welsch, S. Scheel, and A. V. Chizhov, e-print quant-ph/0105111.
[33] A. Erdelyi, W. Magnus, F. Oberhettinger, and F. G. Tricomi, *Higher Transcendental Functions* (McGraw-Hill, New York, 1953), Vol. 2.
[34] V. V. Dodonov and V. I. Man'ko, J. Math. Phys. **35**, 4277 (1994).
[35] C. W. Gardiner, *Quantum Noise* (Springer, Berlin, 1991).